

High-efficiency multilayer-coated ion-beam-etched blazed grating in the extreme-ultraviolet wavelength region

Hui Lin,^{1,*} Lichao Zhang,² Lifeng Li,¹ Chunshui Jin,² Hongjun Zhou,³ and Tonglin Huo³

¹Department of Precision Instruments, State Key Laboratory of Precision Measurement Technology and Instruments, Tsinghua University, Beijing 100084, China

²State Key Laboratory of Applied Optics, Changchun Institute of Optics and Fine Mechanics and Physics, Chinese Academy of Sciences, Changchun 130022, China

³National Synchrotron Radiation Laboratory, University of Science and Technology of China, Hefei 230029, China

*Corresponding author: hui_lin00@mails.tsinghua.edu.cn

Received December 4, 2007; revised January 21, 2008; accepted January 27, 2008;
posted January 29, 2008 (Doc. ID 90465); published February 27, 2008

We describe a simple method to fabricate blazed gratings used in the extreme ultraviolet wavelength region. The method uses an argon and oxygen mixed-gas ion beam to directly etch the grating substrate through a rectangular profile photoresist grating mask. With this method the etched grating groove profile can be well controlled. An Mo/Si multilayer-coated specimen with a blaze angle of 1.9° was fabricated and measured. At an incident angle of 10° and a wavelength of 13.62 nm, the diffraction efficiency of the negative second order reaches 36.2%. © 2008 Optical Society of America
OCIS codes: 050.1950, 120.4610, 310.1620, 340.7480.

Diffraction grating is a key element of extreme-ultraviolet (EUV) spectrometers that are widely used in solar imaging, plasma diagnostics, and so on. To achieve high diffraction efficiency in normal-incidence, a high-reflectance multilayer coating and a high-quality grating groove profile are required. Blazed gratings are in general preferable to laminar gratings in the EUV region. However, the blaze angle required in this spectral region is so small ($<3^\circ$) that it is difficult to precisely control the groove profile. Historically, mechanically ruling blazed gratings were used first but the diffraction efficiencies were below 4% due to ruling errors and surface roughness [1]. Ion-beam-etched holographic gratings are smoother than ruled ones but tend to suffer from a curved blaze facet when the blaze angle is smaller than 6° [2] so that the efficiencies were once limited to 13% [3]. Osterried *et al.* [4] developed a technique in which an ion-beam-etched grating of a relatively large blaze angle ($\sim 7^\circ - 11^\circ$) is dip coated with a liquid polymer, resulting in a reduced blaze angle ($<3^\circ$) with a well-shaped profile. Kowalski *et al.* [5] measured the EUV efficiency of a multilayer grating fabricated by this technique and obtained 29.9% peak efficiency at the wavelength of 15.79 nm.

We have developed an alternative blazed profile shaping method that consists of using an argon and oxygen mixed-gas ion beam to etch a fused silica substrate through a rectangular-profile photoresist grating mask. In this Letter we describe the fabrication process and present our efficiency measurement results of a multilayer-coated grating specimen.

The grating specimen was designed for the negative second order whose peak wavelength is between 13 and 14 nm at 10° incidence. The target grating parameters deduced from the blaze condition are shown in Table 1. We first spin coated the photoresist on a finely polished fused silica substrate of 30 mm

$\times 30$ mm in area and 1 mm in thickness. Then we followed the conventional holographic exposure and development steps to form a 2400 grooves/mm grating mask. Using the nonlinear exposure-development characteristics of the photoresist, we got an etch mask whose ridges are approximately rectangular. After that, we did Ar^+ and O^+ mixed ion-beam etching with a Kaufman ion-beam source. As the target blaze angle is very small, we mounted the specimen on a tilt stage to make the incident ion beam graze the substrate surface (grazing incident angle $<10^\circ$). Since O^+ ions can react with the photoresist, the etch rate ratio of photoresist to fused silica can be significantly enhanced. This characteristic has been used to achieve a blaze angle $<3^\circ$ in gratings etched into a substrate with holographically recorded blazed grating masks [2]. Here we applied it to ion-beam etching with rectangular grating masks to get gratings of a smaller blaze angle than those etched by the previous techniques. Using O^+ ions has another advantage in that their ashing effect can remove some irregularities of the photoresist mask, making the etched blazed profile smoother. We controlled the blaze angle by adjusting the tilt angle of the stage and noticed that the blaze angle was approximately proportional to the grazing incident angle of the ion beam.

The shaping of a blazed profile under ion-beam etching depends on the photoresist mask. In the past, people often used etch masks of approximately a half-sinusoidal shape. The evolution of grating profiles under ion-beam etching was sensitive to the angle at which the mask intercepts the substrate [6]. As it was difficult to precisely control this angle during holographic exposure and development, it was difficult to control the etching process. With the rectangular masks, the photoresist erosion process can be simplified to simultaneous ridge height reduction and width shrinkage at a fixed rate ratio. If the initial

Table 1. Designed and Measured Grating Parameters^a

Parameter Name	Parameter Value		
	Design	Before Coating	After Coating
Groove density (grooves/mm)	2400	2398±1	2398±1
Blaze angle (degrees)	1.81–1.94	1.91±0.07	1.90±0.09
Antiblaze angle (degrees)	~10	8.3±0.5	6.8±1.1
Roughness (nm rms, 2–40 μm^{-1})	<1.0	0.56±0.09	0.50±0.10

^aThe groove density was obtained by measuring the autocollimation diffraction angle of the negative first order at a wavelength of 632.8 nm. The other three parameters were deduced from AFM data.

height and width were properly chosen, we would get a well-shaped blazed profile. As the initial height was determined by the spin-coating parameters and the initial width was controlled by using a development monitoring technique [7], it was convenient to predict the etching process and determine the appropriate etch time.

The multilayer coating composed of 40 periods of an Mo/Si layer pair was deposited onto the bare grating by ion-beam sputtering. The thickness of each layer pair (the period) was 7.1 nm, and the ratio of the Mo thickness to the period was 0.4 so as to achieve maximum reflectance at a wavelength of 13.7 nm at 10° incidence. We determined the period by fitting the small angle x-ray diffraction curve. Its deviation was below 0.03 nm, meeting our design goal.

Atomic force microscopy (AFM) was used to measure the grating profile before and after multilayer coating. Seven locations in or around the specimen center were measured. We used the algorithm introduced in [8] to deduce grating parameters from the AFM data. The blaze and antiblaze angles were computed from a statistics algorithm, and the roughness was calculated by integrating the power spectral density over the range 2–40 μm^{-1} . The parameters averaged over all locations are shown in Table 1. As there are variations in the profile for different AFM images, a typical AFM image before coating and the average profile are illustrated in Fig. 1, where a typical average profile after coating and the theoretically designed profile are also shown.

Efficiency measurements were made at the Spectral Radiation Standard and Metrology Beamline of the National Synchrotron Radiation Laboratory of China. The beamline is equipped with a scanning monochromator that uses a spherical grating with spectral resolution ($\lambda/\Delta\lambda$) of ~192. To suppress the signal of higher harmonics, a filter made of silicon nitride was mounted after the monochromator. The specimen was measured in a reflectometer that allows the specimen holder and the photodiode detector to move in several degrees of freedom. The incident

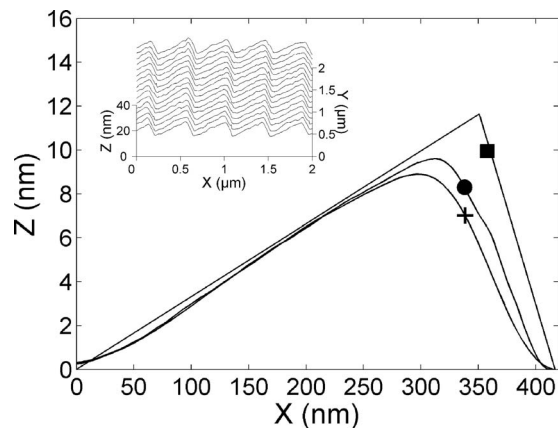


Fig. 1. Typical AFM-measured average groove profile and the designed groove profile. Closed square, designed; closed circle, measured before multilayer coating; plus, measured after multilayer coating. The inset is an AFM image before multilayer coating. The X axis is perpendicular to the orientation of the grating groove, the Y axis is parallel to the groove, and the Z axis is along the normal of the grating plane.

radiation was ~80% s polarization (electric vector parallel to the groove), and the spot size on the grating was 3 mm × 1 mm. A slit of ~0.8 mm in width was mounted in front of the detector to resolve diffraction orders.

We first calibrated the wavelength scale of the monochromator by measuring the Si L absorption edge of the filter. Then we fixed the incident angle to 10° and let the detector scan the diffraction angular spectrum at wavelengths in increments of 0.06 nm from 12.96 to 14.46 nm. As the incident beam intensity might have slightly drifted with time, we measured it at the beginning and end of the 26 scan sequence that lasted ~4 h. The incident beam intensity for each angular scan was obtained by linear interpolation of these two values with respect to the measurement time.

Figure 2 illustrates the angular spectrum of diffraction efficiency measured at the peak wavelength of 13.62 nm for the negative second order, which is a bit different from the peak wavelength of the multilayer reflectance (13.7 nm) due to the slight

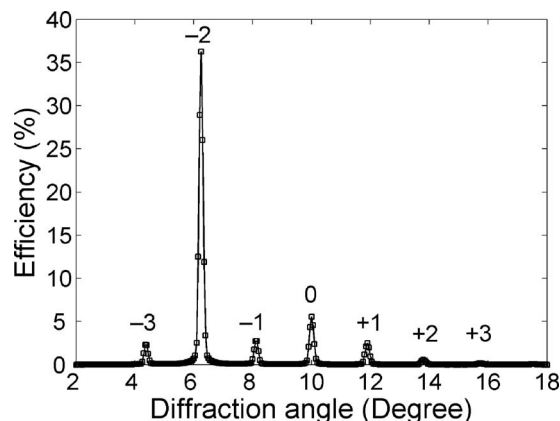


Fig. 2. Diffraction efficiency angular spectrum of the Mo/Si multilayer-coated blaze grating at a 10° incident angle and a 13.62 nm wavelength.

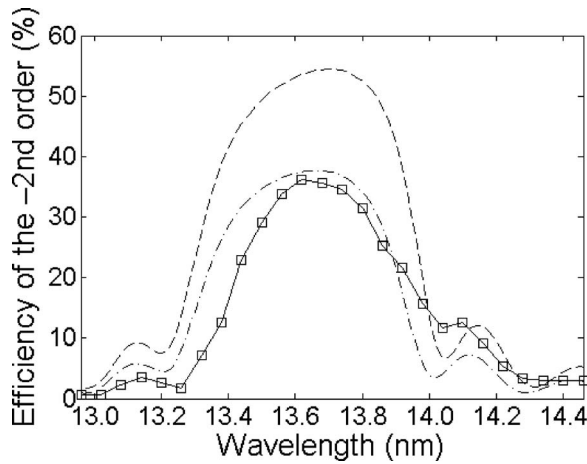


Fig. 3. Measured and calculated negative second-order diffraction efficiencies versus wavelength at an incident angle of 10° . Squared solid curve, measured; dashed curve, calculated, designed ideal groove profile; dashed-dotted curve, calculated, measured actual profile.

mismatch between the blaze angle and multilayer coating. The efficiency of the negative second order is 36.2%. The other diffraction orders are well suppressed, the sum of whose efficiencies is 13.2%, only one third of the negative second-order efficiency. The stray light is much weaker than the diffracted beams, owing to low roughness of the grating profile.

Figure 3 shows the measured and calculated negative second-order diffraction efficiencies versus the wavelength. The theoretical curves were calculated for the designed ideal profile and the measured actual groove profile shown in Fig. 1 by using a code based on the differential theory [9]. In the calculation for the actual groove profile, the profile evolution during multilayer coating and the roughness are taken into account. The measured curve is in good agreement with the calculated ones in both shape and peak position. This demonstrates that the specimen has rendered the desired performance of a multilayer blazed grating.

The high efficiency result is mainly due to our accurate control of the groove profile by using the proposed fabrication technique. First, the blaze angle of the specimen coincides with the design target, well satisfying the blaze condition. Second, the blaze and antiblaze facets are flat, avoiding the curved-facet phenomenon of previous work on small-blaze-angle gratings. Compared with curved facets, flat facets can distribute more incident radiation to the desired order and suppress other orders to a

lower level. Thus, it is one of the key conditions to obtain high efficiency. Last, the roughness is about 0.5 nm rms. As a result, the scattering loss caused by stray light is low.

However, all things considered, there is still a gap between the measured and calculated (ideal) efficiencies. This is mainly because of the rounding effect at the groove edge and the antiblaze angle being smaller than the design value (Fig. 1). These phenomena become more significant after multilayer coating due to the smoothing effect of the coating. They both cause a reduction of the groove height resulting in reduced diffraction efficiency.

In conclusion, we have fabricated an Mo/Si multilayer-coated blazed grating by using a technique that etches fused silica substrates with an Ar^+ and O^+ mixed ion beam through a rectangular photoresist grating mask. The technique is simple and the fabrication process is convenient to control. Owing to the well-controlled groove profile, the peak diffraction efficiency of the negative second order has reached 36.2% at a wavelength of 13.62 nm and an incident angle of 10° . In the future, we will focus our study on reducing the remaining imperfections of the groove profile and thereby obtaining higher diffraction efficiency.

We thank Shu Pei of the State Key Laboratory of Applied Optics of China for the AFM measurements. This Letter was supported by an internal fund of the State Key Laboratory and by the National Natural Science Foundation of China under project 60678034.

References

1. U. Kleineberg, K. Osterried, H.-J. Stock, D. Menke, B. Schmiedeskamp, D. Fuchs, P. Müller, F. Scholze, K. F. Heidemann, B. Nelles, and U. Heinzmann, *Appl. Opt.* **34**, 6506 (1995).
2. B. Nelles, K. F. Heidemann, and B. Kleemann, *Nucl. Instrum. Methods Phys. Res. A* **467–468**, 260 (2001).
3. M. P. Kowalski, T. W. Barbee Jr., R. G. Cruddace, J. F. Seely, J. C. Rife, and W. R. Hunter, *Appl. Opt.* **34**, 7338 (1995).
4. K. Osterried, K. F. Heidemann, and B. Nelles, *Appl. Opt.* **37**, 8002 (1998).
5. M. P. Kowalski, R. G. Cruddace, K. F. Heidemann, R. Lenke, H. Kierey, T. W. Barbee Jr., and W. R. Hunter, *Opt. Lett.* **29**, 2914 (2004).
6. L. F. Johnson, *Appl. Opt.* **18**, 2559 (1979).
7. L. Li, M. Xu, G. I. Stegeman, and C. T. Seaton, *Proc. SPIE* **835**, 72 (1988).
8. M. P. Kowalski, W. R. Hunter, and T. W. Barbee Jr., *Appl. Opt.* **45**, 305 (2006).
9. M. Nevière, *J. Opt. Soc. Am. A* **8**, 1468 (1991).